Journal of the Optical Society of Korea, Vol. 7, No. 3, September 2003, pp. 197-201

Determination of Acceptor Concentration by Use of Recording Dynamics of Photorefractive Holograms Under Low-Intensity Condition in $LiNbO_3$

Bong Gi Kim and Bum Ku Rhee*

Dept. of Physics, Sogang University, Seoul 100-611, KOREA

Seung-Ho Shin

Dept. of Physics, Kangwon National University, Chunchon 200-701, KOREA

(Received February 18, 2003)

We investigated recording dynamics of a holographic grating in the photorefractive $LiNbO_3$ crystal under the low-intensity condition of recording beams. New expressions for the space-charge field and the recording time constant were obtained by solving the Kukhtarev equations under the global space -charge field, which is induced in the previous process of recording and erasing. Their validity can be confirmed by considering the limit that the period of the grating goes to infinity both theoretically and experimentally. It was found that the new expression for the recording time constant allows us to determine acceptor concentration to be $1.2\times10^{21}m^{-3}$ for pure $LiNbO_3$ crystal and $2.5\times10^{21}m^{-3}$ for the 0.1 mol % iron doped $LiNbO_3$ crystal from the measured ratio of the recording time constant under the extremely large grating condition, in which the diffusion effect can be neglected, to that under the small grating condition.

OCIS codes : 090.2900, 090.7330, 160.5320.

I. INTRODUCTION

Photorefractive $LiNbO_3$ crystal is one of the most widely used media for optical storage, image processing, optical computing, and neural networks [1-5]. Hologram recording procedure in the photorefractive crystal can be generally explained in terms of a band transport model developed by Kukhtarev [6]. It is well known that the $LiNbO_3$ crystal has a large photovoltaic effect, which is important among the various transport mechanisms [7,8]. Rupp *et al.* [9] investigated the strongly oxidized $LiNbO_3$:Fe crystals by using a holographic method and observed the enhanced phase shifts between light intensity pattern and refractive index grating due to the low concentration of filled traps. Especially, Gu *et al.* [10] studied the growth of the spatially uniform field across the crystal as a function of time in the fresh crystal. The results obtained by Gu *et al.* clearly showed that the transient behavior of holographic gratings under the open-circuit boundary condition is very different from that under the steady dc voltage (SDCV) condition, which is developed in the previous exposure for recording of the grating. However, they did not study the growth dynamics of holographic gratings under SDCV condition in detail, which might reveal some information on important parameters for photorefractive behavior of the crystal.

In this paper, we solve Kukhtarev equations subject to the SDCV condition in the low-intensity limit of recording beams, and obtain new expressions for the space-charge field and the recording time constant. The new expressions are verified theoretically and experimentally by considering their simplified situation of the large grating limit where the diffusion effect can be neglected. In the experiment, the time dependence of diffraction efficiency was measured as a function of the crossing angle and the intensity of the two recording beams. The experimental results can be explained consistently with the new expressions for the space-charge field and recording time constant, leading to the determination of conductivities. We show that the acceptor concentration in $LiNbO_3$ doped with Fe as well as pure $LiNbO_3$ can be determined by comparing the ratio of the recording time constant under the extremely large grating to that under the small one.

II. RECORDING DYNAMICS OF $LINBO_3$ CRYSTAL UNDER THE LOW-INTENSITY CONDITION

The band transport model can be described by the following set of equations developed by Kukhtarev:

$$\frac{\partial N_D^+}{\partial t} = (N_D - N_D^+)(sI + \beta) - \gamma_R n_e N_D^+ \quad , \tag{1}$$

$$\frac{\partial n_e}{\partial t} = \frac{\partial N_D^+}{\partial t} + \frac{1}{e}\frac{\partial J}{\partial x} \quad , \tag{2}$$

$$J = e\mu n_e E + k_B T \mu \frac{\partial n_e}{\partial x} + pI \quad , \tag{3}$$

$$\epsilon \frac{\partial E}{\partial x} = e(N_D^+ - n_e - N_A) \quad , \tag{4}$$

where N_D, N_D^+, n_e, and N_A are densities of filled traps, ionized traps, charged carriers and acceptors, respectively,. In the above equations, s is the photoexcitation cross section, I is the total optical intensity, β is the thermal generation rate of charge carriers, γ_R is the carrier recombination rate, e is the electronic charge, μ is the carrier mobility, k_B is Boltzmann's constant, p is the photovoltaic constant, ϵ is the dielectric constant of the crystal, and E is the total electric field inside the crystal.

Before solving Kukhtarev equations, the proper expressions for the photovoltaic current and the conduction current in Eq. (3) need to be considered under the low-intensity condition of the recording beams. At first, a typical expression for the photovoltaic term is given as either pI or $p(N_D - N_D^+)I$ according to the references of [10-12]. Here pI is used because a change of N_D^+ due to a light illumination is much smaller than the initial value of N_D^+ and N_D under a low-intensity condition. Thus the photovoltaic current is directly proportional to the optical intensity distribution, which is given by $I = I_0 + I_1 \cos(Kx)$, where K is the grating wave vector. Secondly, the dark conductivity (σ_d) has to be considered with the photoconductivity (σ_{ph}), because the photoconductivity could be low under a low-intensity condition as far as conductivity is concerned [13]. When the grating is recorded and erased by non-Bragg matched beam, uniform electric field , $E_0 = E_{ph} = -pI_0/\sigma_{ph}$, remains across the region where the hologram was written (SDCV condition) [10]. By the presence of this field, the photovoltaic current can not flow during the second recording so that there is no contribution of the dc component to the current density in Eq. (3). Therefore, the correct expression for the current density under this SDCV condition should be as follows;

$$J = J_1 = (\sigma_d + \sigma_{ph})E_1 + iKk_B T\mu n_{e1} + pI_1 \quad , \tag{5}$$

where n_{e1} and E_1 are the modulated component of the density of charge carriers and the space-charge field, respectively.

Eqs. (1), (2), (4), and (5) can be solved with the standard linearization procedure using first order perturbation under the condition of a small modulation ratio, i.e., $m = I_1/I_0 << 1$. After some algebraic manipulations, the solution for the space-charge field, E_{sc}, is given by

$$E_{sc}(z,t) = -mE_{sc}^o[1 - exp(-\frac{t}{\tau_g})]cos(Kz + \phi) \quad , \tag{6}$$

where τ_g is the recording time constant and ϕ is the phase shift of the refractive index grating with respect to the periodic light intensity pattern. The saturation space-charge fields E_{sc}^o and the time constant τ_g are given by

$$E_{sc}^o = E_q \frac{\sqrt{E_{ph}^2 + E_d^2}}{(E_d + E_q - \frac{\sigma_d}{pI_0}E_q E_{ph})} \quad , \tag{7}$$

$$\frac{1}{\tau_g} = \frac{1}{\tau_{di}}\frac{(1 + \frac{E_d}{E_q})}{(1 + \frac{E_d}{E_\mu})} + \frac{\frac{\sigma_d}{\epsilon}}{1 + \frac{E_d}{E_\mu}} \quad . \tag{8}$$

In Eqs. (7) and (8), we have used the expressions for the dielectric relaxation time(τ_{di}), the diffusion field(E_d), the saturation field(E_q), the drift field(E_μ) and the photovoltaic field(E_{ph}) as follows:

$$\tau_{di} = \frac{\epsilon}{e\mu n_{e0}} = \frac{\epsilon}{e\mu}\frac{\gamma_R N_A}{(N_D - N_A)sI_0} \quad ,$$

$$E_d = \frac{k_B T K}{e} \quad ,$$

$$E_q = \frac{eN_A(N_D - N_A)}{\epsilon K N_D} \quad ,$$

$$E_\mu = \frac{\gamma_R N_A}{\mu K} \quad ,$$

$$E_{ph} = -\frac{p\gamma_R N_A}{e\mu s(N_D - N_A)} \quad .$$

It should be noted that the photovoltaic term on the space-charge field more clearly appears in the numerator of Eq. (7) compared with the corresponding result obtained by Gu *et al.* [10]. The validity of Eqs. (7) and (8) can be confirmed by considering the limit that K goes to zero (the large grating limit) so that diffusion effect can be neglected (E_d=0), reducing to the following simplified expressions;

$$E_{sc}^{o} = -\frac{pI_0}{\sigma_d + \sigma_{ph}} \quad , \tag{9}$$

$$\tau_g = \frac{\epsilon}{\sigma_d + \sigma_{ph}} \quad , \tag{10}$$

where $\epsilon=\epsilon_s\epsilon_o$, ϵ_s is the relative dielectric constant of the medium, and $\epsilon_o=8.85\times10^{-12}C^2/Nm^2$. As expected, these results are exactly same as the corresponding results [14] for the photorefractive index change under the uniform illumination with a single recording beam.

III. EXPERIMENTS

The experiments were performed with a two-wave mixing scheme as shown in Fig. 1. Two Ar-ion laser beams ($\lambda = 514.5nm$), which were divided by a beam splitter, interfered inside the crystal to form a sinusoidal grating. We used ordinary polarized recording beams to minimize the beam coupling effect, and the intensity ratio of the two recording beams was made to realize the small modulation ratio of 1/3. A non-Bragg matched beam was employed for erasing the grating after the first recording, as shown in Fig. 1. The He-Ne laser beam ($\lambda = 632.8nm$), which is extraordinarily polarized, was used to utilize the large r_{33} electro-optic coefficient for detecting a space-charge field which is induced inside the crystal during the recording process. Two different types of $LiNbO_3$ crystals were investigated in the experiment; one is the nominally pure lithium niobate (congruent $LiNbO_3$; $1.54\times10\times4.55$ mm^3[abc-axis]) and the other is the lithium niobate doped with 0.1 mole% Fe ($LiNbO_3$:Fe; $1.58\times10\times4.61$ mm^3[abc-axis]).

To analyze the experimental results obtained under the various conditions consistently, the modulation ratio (1/3) and the intensity of the reading beam

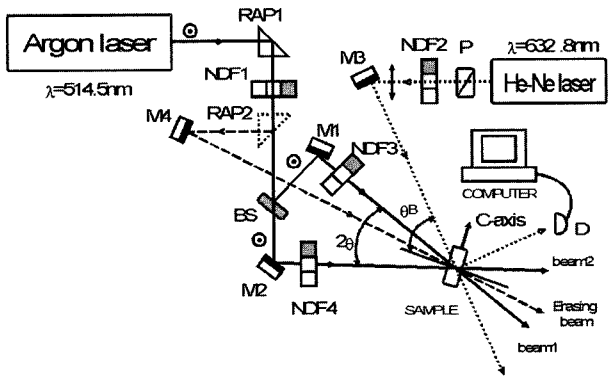

FIG. 1. Schematic diagram of experimental setup for holographic recording and reading system; P: polarizer, RAP: right angle prism, M: mirror, ND: neutral density filter, BS: beam splitter, and D: detector.

($1mW/cm^2$) were kept the same for all experiments. Hologram recording experiments were carried out under two extremely different crossing angles of the two recording beams; i.e., $2\theta=60^o(\Lambda = 0.51\mu m$; small grating) and $2\theta=8^o(\Lambda = 3.69\mu m$; large grating). The crystal was regularly cleaned at 190^oC for five hours in a hot oven in order to restore its virgin condition. After the first recording, only the hologram was erased optically using a non-Bragg matched erasing beam. Then, during the period of the second recording process, the diffraction efficiency was measured as a function of recording time by use of a weak He-Ne laser beam to characterize Eq. (6).

IV. DISCUSSION

The typical curves of the diffraction efficiency measured as a function of the recording time are shown in Fig. 2(a) under the large grating condition and Fig. 2(b) under the small grating condition for pure $LiNbO_3$. Each experiment was performed with recording beams of different intensities; i.e., I_0=5.1W $/cm^2$(o) and I_0=10.2W/cm^2(□). The same experi-

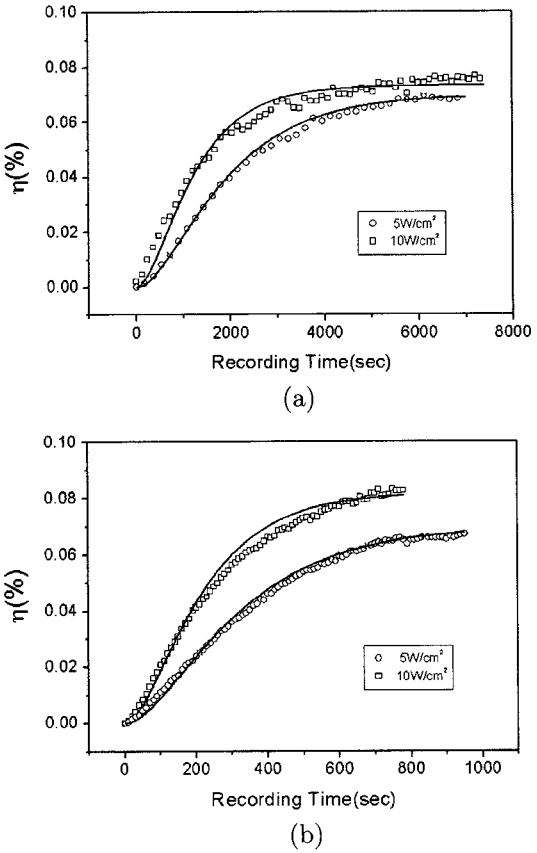

FIG. 2. Evolution of diffraction efficiencies for $LiNbO_3$ with 5.1W/cm^2(o) and 10.2W/cm^2(□); (a) under the large grating condition (Λ=3.69μm), and (b) under the small grating condition (Λ=0.51μm). Solid curves are the best fitting using $\eta = \sin^2[\eta_0(1 - exp(-t/\tau_g)]$.

TABLE 1. Conductivities, Cross sections, and Acceptor concentrations determined from experimental results

	σ_d $(\Omega\ \mathrm{cm})^{-1}$ $\times 10^{-16}$	$\mathcal{S}$ $(\frac{\mathrm{cm}}{\Omega W})$ $\times 10^{-16}$	$N_A(\mathrm{m}^{-3})$ $\times 10^{21}$
$LiNbO_3$	5.6 ± 0.2	2.9 ± 0.3	1.2 ± 0.2
$LiNbO_3$:Fe	8.9 ± 0.4	111 ± 17	2.5 ± 0.4

ments were also carried out with $LiNbO_3$:Fe and the corresponding results are shown in Fig. 3(a) under the large grating condition and Fig. 3(b) under the small grating condition. Here, two different intensities of recording beams for $LiNbO_3$:Fe are I_0=30mW/cm^2(○) and I_0=60mW/cm^2(□). This significant difference in I_0 between $LiNbO_3$ and $LiNbO_3$:Fe is due to the fact that the photovoltaic constant for $LiNbO_3$:Fe is much larger than that for $LiNbO_3$ [7]. The solid curves in Figs. 2 and 3 are obtained by the best fitting with $\eta = \sin^2[\eta_0(1 - exp(-t/\tau_g)]$ [15], yielding the best fit values of τ_g. From these results, one can find that τ_g depends strongly on the crossing angle, but only slightly on I_0 for $LiNbO_3$ while τ_g depends strongly on both the crossing angle and I_0 for $LiNbO_3$:Fe.

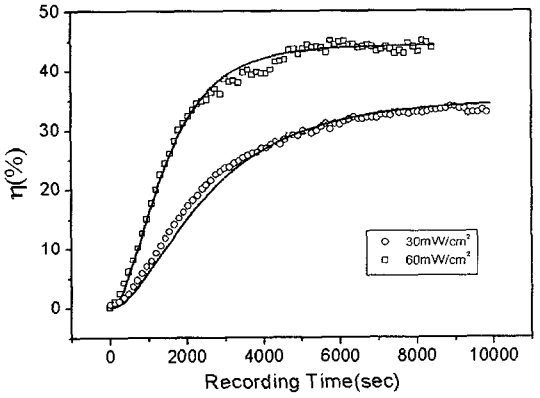

(a)

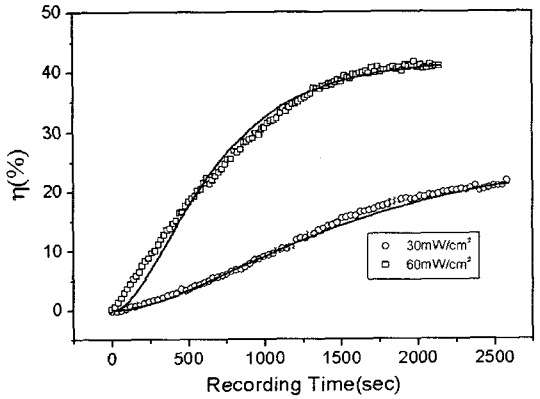

(b)

FIG. 3. Evolution of diffraction efficiencies for $LiNbO_3$:Fe with 30mW/cm^2(○) and 60mW/cm^2(□); (a) under the large grating condition(Λ=3.69μm), and (b) under the small grating condition (Λ=0.51μm). Solid curves are the best fitting using $\eta = \sin^2[\eta_0(1 - exp(-t/\tau_g)]$.

In our experiment, E_d under the large grating condition is so small that it can be neglected. Therefore, σ_d and σ_{ph} can be determined by using two coupled equations, Eq. (10) and $\sigma_{ph} = \mathcal{S}\ I_0$, where $\mathcal{S}$ is the cross section for the photoexcitation, with the best-fit values of two time constants corresponding to two different conditions of I_0 obtained from Fig. 2(a) for $LiNbO_3$ and Fig. 3(a) for $LiNbO_3$:Fe. The values obtained for conductivities are listed in Table 1, which are of the same order of those measured directly using an electrometer [16]. Here ϵ_s=32 is used [17]. Note should be taken that $\sigma_d \ll \sigma_{ph}$ for $LiNbO_3$ while $\sigma_d \simeq \sigma_{ph}$ for $LiNbO_3$:Fe under our illumination condition. Thus one can expect easily from Eq. (9) that the saturation diffraction efficiency, which is proportional to $\sin^2(constant \times E_{sc}^o)$, depends strongly on I_0 for $LiNbO_3$: Fe under the large grating condition. These expectations can be clearly confirmed from the corresponding experimental results shown in Fig. 3(a) while the saturation diffraction efficiency is approximately independent of I_0 for $LiNbO_3$ as shown in Fig. 2(a).

Furthermore, it is generally known that $E_\mu \gg E_d$ and $N_A \ll N_D$ [10,18]. Therefore, the τ_g for the small grating ($\tau_{S.G.}$) is given by

$$\frac{1}{\tau_{S.G.}} = \frac{1}{\tau_{di}}(1 + \frac{E_d}{E_q}) + \frac{\sigma_d}{\epsilon} \qquad (11)$$

From Eqs. (10) and (11), it is possible to obtain the ratio of τ_g for the large grating ($\tau_{L.G.}$) to $\tau_{S.G.}$ for the small grating under the same I_0 as follows

$$\frac{\tau_{L.G.}}{\tau_{S.G.}} = 1 + \frac{\sigma_{ph}}{\sigma_d + \sigma_{ph}}\frac{E_d}{E_q} \simeq 1 + \frac{\sigma_{ph}}{\sigma_d + \sigma_{ph}}\frac{\epsilon k_B T K^2}{e^2 N_A} \quad . \quad (12)$$

By using Eq.(12) with the numerical values obtained for σ_d and σ_{ph} listed in Table 1, one can determine the acceptor concentration to be $(1.2\pm0.2)\times10^{21}\mathrm{m}^{-3}$ for pure $LiNbO_3$ and $(2.5\pm0.4)\times10^{21}\mathrm{m}^{-3}$ for $LiNbO_3$:Fe. We found that these values of N_A, listed in Table 1, are comparable to the result obtained by Tyminski *et al.* [19] using the holographic grating-decay pattern measurements in pure $LiNbO_3$, and are much smaller than a known donor density of the order of $10^{24}/\mathrm{m}^3$ in $LiNbO_3$:Fe [20].

V. CONCLUSION

In conclusion, we have solved Kuktahrev equations by taking account of not only the steady dc voltage but also the low-intensity of the recording beams. The modified expressions for the space-charge field and the recording time constant are derived. In order to verify these modified expressions, we performed holographic recording experiments as a function of the various crossing angles and intensities of two recording beams. It was found that experimental results can be explained consistently by using modified expressions, yielding the numerical values of conductivities from the intensity dependence of τ_g under the extremely large grating condition in which diffusion effects can be neglected. We have also demonstrated that the acceptor concentration can be determined by using the ratio of two recording time constants under the extremely large grating and the small grating with the corresponding prediction. We believe that these modified expressions for the space-charge field and the recording time constant under the steady dc voltage condition should be useful in explaining the photorefractive hologram recording mechanism with photovoltaic effect.

ACKNOWLEDGEMENTS

This study was funded by Dankook Medical Laser Research Ceneter (R12-2001-050-05002-0(2002)).

*Corresponding author : brhee@ccs.sogang.ac.kr.

REFERENCES

[1] L. Hesselink and L. M. C. Bashaw, "Optical memory implemented with photorefractive media," *Optical and Quantum Electronics*, vol. 25, pp. S611-S661, 1993.

[2] F. H. Mok, G. W. Burr and D. Psaltis, "System metric for holographic memory system," *Opt. Lett.*, vol. 21, no. 12, pp. 896-898, 1996.

[3] T. Y. Chang, P. H. Beckwith, and P. Yeh, "Real-time optical image subtraction using dynamic holographic interference in photorefractive media," *Opt. Lett.*, vol. 13, no. 7, pp. 586-588, 1988.

[4] C. Gu, S. Campbell, and P. Yeh, "Matrix-matrix multiplication by using grating degeneracy in photorefractive media," *Opt. Lett.*, vol. 18, no. 2, pp. 146-148, 1993.

[5] D. Psaltis, D. Brady, X. G, Gu, and L. Lin, "Holography in artificial neural networks," *Nature*, vol. 343, pp. 325-330, 1990.

[6] N. V. Kukhtarev, V. B. Markov, S. G. Odulov, M. S. Soskin, and V. L. Vinetskii, "Holographic storage in electrooptic crystals. I. steady state," *Ferroelectrics*, vol. 22, pp. 949-960, 1979.

[7] A. M. Glass, "The photorefractive effect," *Opt. Eng.*, vol. 17, pp. 470-479, 1978.

[8] A. M. Glass, D. von der Linde, and T. J. Negran, "High-voltage bulk photovoltaic effect and the photorefractive process in $LiNbO_3$," *Appl. Phys. Lett.*, vol. 25, pp. 233-235, 1974.

[9] R. A. Rupp, R. Sommerfeldt, K. H. Ringhofer, and E. Krätzig, "Space charge field limitations in photorefractive $LiNbO_3$:Fe crystals," *Appl. Phys.*, vol. B51, pp. 364-370, 1990.

[10] C. Gu, J. Hong, H.-Y, Li, D. Psaltis, and P. Yeh, "Dynamics of grating formation in photovoltaic media," *J. Appl. Phys.*, vol. 69, no. 3, pp. 1167-1172, 1991.

[11] D. K. McMillen, T. D. Hudson, F. T. S. Yu, T. Zhang, S. Yin, and Z. Wu, "Anomalies of photovoltaic current in a Cd:Fe doped $LiNbO_3$ crystal at 55 and 75 temperatures," *Opt. Eng.*, vol. 34, no. 8, pp. 2240-2242, 1995.

[12] M. Simon, S. Wevering, K. Buse, and E. Krätzig, "The bulk photovoltaic effect of photorefractive $LiNbO_3$:Fe crystals at high light intensities," *J. Phys. D:Appl. Phys.*, vol. 30, no. 1, pp. 144-149, 1997.

[13] B. G. Kim and B. K. Rhee,"Determination of photovoltaic constant and photoconductivity in $LiNbO_3$:Fe using Maker fringes," Opt. Commun., vol. 198, pp. 193-197, 2001.

[14] R. Grousson, M. Henry, S. Mallick, and S. L. Xu, "Measurement of bulk photovoltaic and photorefractive characteristics of iron doped $LiNbO_3$," *J. Appl. Phys.*, vol. 54, no. 6, pp. 3012-3016, 1983.

[15] H. Kogelnik, "Coupled-wave theory for thick holographic gratings," *Bell Sys. Tech. J.*, vol. 48, pp. 2909-2947, 1969.

[16] W. Huafu, S. Guotong, and W. Zhongkang, "Photovoltaic effect in $LiNbO_3$:Mg," *Phys. Stat. Sol.(a)*, vol. 89, no. 2, pp. K211-k213, 1985.

[17] F. Jermann, M. Simon, and E. Krätzig, "Photorefractive properties of congruent and stoichiometric lithium niobate at high light intensities," *J. Opt. Soc. Am. B*, vol. 12, no. 11, pp. 2066-2070, 1995.

[18] S. H. Lin, M. L. Hsieh, K. Y. Hsu, T. C. Hsieh, S.-P. Lin, T.-S. Yeh, L.-J. Hu, C.-H. Lin, and H. Chang,"Photorefractive Fe:$LiNbO_3$ crystal thin plates for optical information processing," *J. Opt. Soc. Am. B*, vol. 16, no. 7, pp. 1112-1119, 1999.

[19] J. K. Tyminski, and R. C. Powell, "Analysis of the decay dynamics of laser-induced gratings in $LiNbO_3$," *J. Opt. Soc. Am. B*, vol. 2, no. 3, pp. 440-446, 1985.

[20] F. Jermann and J. Otten, "Light-induced charge transport in $LiNbO_3$:Fe at high light intensities," *J. Opt. Soc. Am. B*, vol. 10, no. 11, pp. 2085-2092, 1993.